ORIGINAL ARTICLE

The Effect of Heterogeneity in Small Electron Fields: A Dosimetric Study

Sara Shomal-Nasab [1], Hossein Sadeghi [1], Fatemeh Seif [2*], Mohammad Reza Bayatiani [2]

[1] *Department of Physics, Faculty of Sciences, Arak University, Arak, Iran*

[2] *Department of Radiotherapy and Medical Physics, Arak University of Medical Sciences & Khansari Hospital, Arak, Iran*

*Corresponding Author: Fatemeh Seif

Email: sahar_s59@yahoo.com

Received: 04 June 2025 / Accepted: 03 November 2025

Abstract

Purpose: Small electron fields are used in radiotherapy for superficial tumors and areas close to the skin. However, the impact of tissue heterogeneity on dose distribution in these fields poses considerable challenges. To explore how the variability of cold foam affects dose distribution in small electron fields using Semiflex 3D and Advanced Markus dosimeters.

Materials and Methods: Dosimetric measurements were performed using an Elekta Vera-HD linear accelerator with 10-MeV and 12-MeV electron beams. Square field sizes of 2×2, 3×3, 4×4, 5×5, and 6×6 cm² were investigated. Dose distributions were assessed using Semiflex 3D and Advanced Markus ionization chambers. Percentage Depth Dose (PDD) curves were analyzed, revealing that at 10 MeV, the depth of maximum dose (d_{max}) was 2.2 cm, while at 12 MeV, it increased to 2.7 cm.

Results: The results confirm that the OF increases with both field size and beam energy. Larger field sizes enhance lateral electron scattering, and higher beam energy enables deeper penetration and broader dose distribution, further increasing the OF. A minimum field size of 3 cm × 3 cm is recommended, as differences between dosimeters were observed in 2 cm × 2 cm and 3 cm × 3 cm fields, but remained below 2% for larger fields. The study also found that increasing heterogeneity reduces the OF, with air-equivalent heterogeneities consistently decreasing the OF across all field sizes and energy levels.

Conclusion: Monte Carlo algorithms in Treatment Planning Systems (TPS) model heterogeneities using CT images and Hounsfield Unit (HU) values. However, their accuracy depends on CT image quality and device calibration, and HU-to-parameter conversion may not fully account for tissue variability. Combining computational simulations with experimental validation is recommended to improve TPS accuracy, especially in electron mode and when dealing with heterogeneities.

Keywords: Tissue Heterogeneity; Small Electron Fields; Radiotherapy; Semiflex 3D; Advanced Markus.

DOI:

1. Introduction

In recent years, electron beams have become a preferred modality for treating superficial lesions, offering a targeted radiation dose with minimal deep tissue penetration. Compared to low-energy X-rays, electron beam therapy provides a more favorable dose distribution for surface tumors, making it especially suitable for lesions in critical regions such as the eyes and lips [1, 2]. The unique dosimetric profile of electron beams, including steep dose gradients and rapid fall-off, helps minimize radiation exposure to adjacent normal tissues [3].

A significant advantage of electron beams is their ability to deliver high surface doses while protecting deeper tissues. This advantage is especially important in cases where oblique photon beams may irradiate more normal tissue than necessary, such as when treating thyroid or breast tumors. The energy of an electron beam is typically selected to ensure that the therapeutic range, defined by the depth corresponding to 90% of the maximum dose (R_{90}), covers the tumor bed. However, R90 is influenced by field size, increasing until a saturation point is reached for fields larger than approximately 10×10 cm² [4]. Moreover, recent advances such as Modulated Electron Radiation Therapy (MERT) allow better control of dose distributions using conformal and small fields [5].

However, delivering accurate doses in small electron fields presents considerable challenges. These include high dose gradients, lateral electron disequilibrium, and the dosimetric influence of tissue heterogeneities such as bone, fat, and air cavities [6, 7]. These heterogeneities affect electron scattering and stopping power, leading to localized hot and cold spots. The impact is particularly pronounced in small fields, where the balance of lateral scattering can be significantly altered. For instance, a high-density heterogeneity can increase scattering and create hot spots near its edges, while low-density regions such as air cavities may lead to dose reductions in their vicinity [8].

While several studies have addressed heterogeneity effects in photon or large electron fields, limited data exist on the dosimetric behavior of small electron fields in the presence of low-density heterogeneities, especially with regard to their effect on output factors (OFs). Furthermore, comparative performance analysis of dedicated small-field dosimeters under these complex conditions has not been sufficiently explored. This study introduces a novel experimental model simulating facial heterogeneity using cold foam, aiming to bridge this gap.

This work focuses on small electron fields (2×2–6×6 cm²) used in treating superficial tumors of the head and face, particularly squamous cell carcinomas. In clinical settings, small cutouts within standard applicators are often employed to shape electron fields, particularly in irregular anatomical regions such as the nose, cheek, lips, and ear, where air gaps and soft tissue variations are common. As direct in vivo dose measurements are not feasible, body-equivalent phantoms must be used for dosimetry.

Although heterogeneity effects in electron dosimetry have been reported previously, our study adds novelty by focusing on very small fields (2×2–6×6 cm²), using cold foam to realistically simulate facial air cavities, and providing a direct comparison of Semiflex 3D and Advanced Markus chambers under identical heterogeneous conditions. These aspects offer new quantitative insights for small-field electron dosimetry in clinically relevant scenarios.

In this study, a cold foam material (density ≈ 0.001 g/cm³) is employed to simulate low-density heterogeneities encountered in superficial facial regions. Foam layers of varying thickness (0, 0.5, 1, and 2 cm) were introduced into a solid phantom to create air-like heterogeneity, and dose measurements were performed at d_{max} depth using electron beams of 10 MeV and 12 MeV. The output factors were measured using two high-resolution dosimeters—Advanced Markus and Semiflex 3D chambers—selected for their suitability in small-field electron dosimetry.

By examining how two important and widely used dosimeters in clinical electron dosimetry respond under different heterogeneity scenarios, the study provides novel insights into dosimetric accuracy in small-field electron therapy. Traditionally, parallel-plate ionization chambers have been used for electron dosimetry; however, nowadays, small-volume dosimeters, especially for small field dosimetry, are preferred. Therefore, we selected the Semiflex 3D

dosimeter due to its small sensitive volume and suitability for small field measurements.

The remainder of this paper is structured as follows: Section 2 describes the materials and methods, including equipment, dosimeters, phantom setup, and measurement procedures. Section 3 presents the results and discussion, highlighting the effects of cold foam heterogeneity on dose distribution and dosimeter response. Finally, Section 4 concludes with a summary of key findings, clinical implications, and recommendations for future research.

2. Materials and Methods

2.1. Dosimeters

In this study, two types of dosimeters, the Semiflex 3D and Advanced Markus, produced by PTW, were utilized to assess dose distribution in heterogeneous materials. Both dosimeters were operated at a bias voltage of +300 V. Table 1 presents a comparison of their specifications. The Semiflex 3D dosimeter is known for its high sensitivity and compact volume (0.07 cm^3), which makes it highly suitable for accurate measurements in all fields ranging from 3×3 cm^2 (small fields) to 40×40 cm^2 (large fields) at energies between 9 and 45 MeV. In contrast, the Advanced Markus dosimeter with a smaller sensitive volume of 0.02 cm^3 is specifically designed for precise surface-dose measurements and is widely used in clinical environments for electron energies between 2 and 45 MeV. Before their use in this study, both dosimeters were calibrated at the Secondary Standard Dosimetry Laboratory (SSDL), and official calibration certificates were issued. The calibration factors provided by SSDL were applied in all subsequent dose measurements to ensure traceability to international standards. In addition, beam output calibration of the Elekta Versa-HD linear accelerator was performed in our clinic according to standard protocols, with cGy/MU set to unity under reference conditions (SSD = 100 cm, 10 × 10 cm^2 field size, and d_{max} for the respective energies). To further ensure accuracy, stability, and leakage tests of the electrometer (PTW, UNIDOS E) were performed prior to data collection, and daily constancy checks were confirmed within ±0.5%.

2.2. Phantom and Heterogeneity

For phantom setup, solid water slabs (PTW, Freiburg, Germany) were stacked on the treatment couch to achieve the required build-up and backscatter conditions. The phantoms were aligned with room lasers to ensure reproducible positioning, and the SSD was carefully verified using the front pointer of the linear accelerator. The foam heterogeneity was inserted at the predetermined location within the slabs, directly above the sensitive volume of the dosimeter, to simulate superficial air cavities under clinically relevant conditions. All setups were independently checked by two medical physicists before measurements to minimize setup errors.

For the material selection process, CT scan assessments were performed (Figure 1). The electron density and Hounsfield units (HU) of these materials were analyzed to identify the most suitable one for creating heterogeneity (Table 2). Based on this analysis, foam was selected due to its favorable electron density and HU, making it ideal for this research. This choice aims to enhance the accuracy and reliability of the study's findings.

CT calibration was performed according to standard protocols to ensure accurate HU values, and HU-to-electron density conversion was verified using tissue-equivalent reference materials. The foam material, with HU ≈ -980 and electron density ≈ 0.001 g/cm^3, closely mimics air in superficial facial regions, ensuring the clinical relevance of the heterogeneity model.

An Elekta Versa-HD linear accelerator operating at energies of 10 and 12 MeV was used in this study. Solid phantoms provided by PTW were employed for the measurements. To evaluate the effect of heterogeneous materials on dose distribution, foam with a density of 0.001 g/cm^3 was used to represent

Table 1. Characteristics of the Advanced Markus and Semiflex 3D PTW dosimeters

Dosimeter/specifications	Field size	Energy	Sensitive volume
Semiflex 3D	3×3 cm^2 to 40×40 cm^2	9-45 MeV	0.07 cm^3
Advanced Markus	3×3 cm^2 to 40×40 cm^2	2-45 MeV	0.02 cm^3

Table 2. Summary of CT scan assessments for material selection as air heterogeneities. (*The mean ED & HU of air in the patient's face lesions was derived from Monaco TPS)

Quantity/Material	Foam	Dry gas	Wet gas	Bolus	Plastic tube	Cork	Cotton	Air in the patient's face lesions*
ED (Electron Density) (e/cm³)	0.001	0.170	1.020	1.185	0.950	0.230	0.040	0.001
HU	-980	-870	0.4	-220	-50	-550	-900	-979

superficial air heterogeneity in head and face lesions (e.g., lesions in the ears, nose, etc.), as illustrated in Figure 2. These slab phantoms were designed to mimic the properties of human tissue, ensuring that the experimental setup closely mirrored the clinical conditions. The foam material was specifically chosen to address clinical challenges where variations in tissue density can significantly affect dose distribution.

Figure 1. Setup of air heterogeneity and dosimeters within solid phantoms

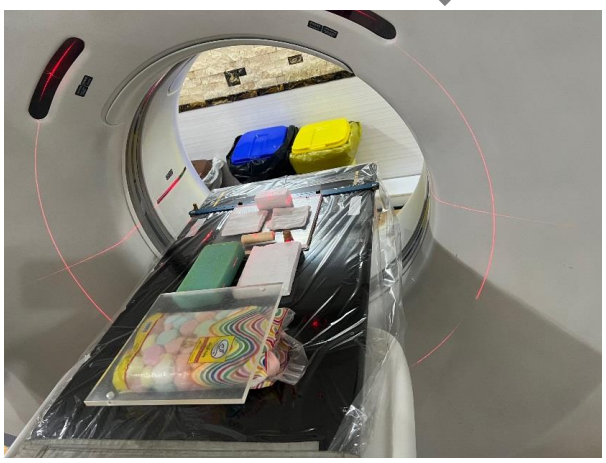

Figure 2. Material selection workflow guided by CT scan assessments

2.3. Measurements

Small fields measuring 2×2, 3×3, 4×4, 5×5, and 6×6 cm² were created using a square applicator that measured 6×6 cm². To create smaller radiation fields, particularly those measuring less than 6 cm, we employed Cerrobend cutouts within a 6x6 cm² applicator. Cerrobend was selected for its excellent shielding capabilities, which helped us achieve precise and effective field shaping. This approach enabled us to accurately target the intended areas while reducing exposure to surrounding tissues. Utilizing Cerrobend cutouts in the 6×6 cm² applicator turned out to be an effective technique for generating smaller, well-defined radiation fields, thereby improving the overall precision and effectiveness of our treatment strategy, as shown in Figure 3.

The Source-to-Surface Distance (SSD) was maintained at 100 cm for all measurements. The d_{max} at 10 and 12 MeV was determined by analyzing the PDD curves. The dosimeters were then placed within the phantoms at the identified d_{max} depth. Heterogeneity was applied to the dosimeter.

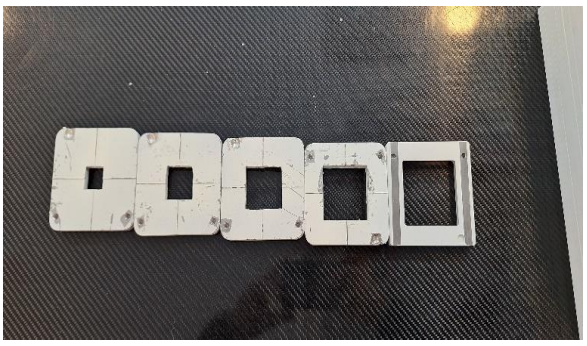

Figure 3. Square Cerrobend Electron Cutouts ranging from 2 cm to 6 cm

2.3.1. Charge Readouts Measurement

The collected charge after introducing heterogeneity was recorded using the electrometer (PTW, UNIDOS E) connected to the dosimeter. The

measurements were repeated three times for each field size, with 100 Monitor Units (equivalent to 100 cGy) for each reading.

2.3.2. OF

The OF is defined as the ratio of the dosimeter reading under specific non-reference conditions to the reading obtained under reference conditions [9]. In this study, the OF is defined as the ratio of the reading in the field created by the cutout to the reading in the reference 6×6 cm² applicator.

A comparative analysis between the readout of Semiflex 3D and Advanced Markus dosimeters was performed.

3. Results

The collected data were analyzed statistically to evaluate the effectiveness of the dosimeters and the effect of air heterogeneity on dose distribution.

3.1. Charge Readouts

The effect of air heterogeneity was evaluated by placing both the Advanced Markus and Semiflex 3D dosimeters under conditions with and without heterogeneity. Measurements were conducted for heterogeneity thicknesses of 0.5 cm, 1 cm, and 2 cm at two energy levels, 10 MeV and 12 MeV. In each case, the charge was measured using an electrometer, and the results are presented in Tables 2–5.

To provide a more robust statistical analysis, all charge measurements reported in Tables 3–6 represent the mean of three repeated measurements (n = 3), rounded to the nearest integer, with the relative standard deviation (SD) reported as ±2%. Paired Student's t-tests were conducted for each combination of energy, field size, and inhomogeneity, with a two-sided p-value < 0.05 considered statistically significant.

3.2. OFs

The OF values, measured with Semiflex 3D and Advanced Markus across all cutouts at 10,12 Mev electron beam energies in a slab phantom at SSD = 100 cm, are presented in Table 6. The symbol Δ (%) represents the percentage difference between the outputs measured by the Advanced Markus and Semiflex 3D dosimeters.

3.3. OF Dependence on Field Size and Inhomogeneity

The comparison of Advanced Markus and Semiflex 3D measurements of OF as a function of field size is shown in the graphs of Figure 4.

Table 3. Charge readout (nC) by the Semiflex dosimeter at 10 MeV energy. (Values are the mean of three repeated measurements (n = 3), rounded to the nearest integer, relative standard deviation (SD= ± 2%).)

Depth of measurement point (cm)	Field size (cm²) / Inhomogeneity (cm)	2×2	3×3	4×4	5×5	6×6
2.2	**0**	921	1170	1299	1368	1375
2.7	**0.5**	690	992	1177	1286	1332
3.2	**1**	506	797	1012	1152	1226
4.2	**2**	375	631	848	1006	1106

Table 4. Charge readout (nC) by the Semiflex dosimeter at 12 MeV energy. (Values are the mean of three repeated measurements (n = 3), rounded to the nearest integer, relative standard deviation (SD= ± 2%).)

Depth of measurement point (cm)	Field size (cm²) / Inhomogeneity (cm)	2×2	3×3	4×4	5×5	6×6
2.7	**0**	850	1132	1287	1370	1386
3.2	**0.5**	629	945	1145	1275	1333
3.7	**1**	465	752	975	1131	1217
4.7	**2**	344	587	806	973	1083

Table 5. Charge readout (nC) by the Advanced Markus dosimeter at 10 MeV energy. (Values are the mean of three repeated measurements (n = 3), rounded to the nearest integer, relative standard deviation (SD= ± 2%).)

Depth of measurement point (cm)	Field size (cm^2) / Inhomogeneity (cm)	2×2	3×3	4×4	5×5	6×6
2.2	**0**	405	486	531	556	580
2.7	**0.5**	314	414	475	514	529
3.2	**1**	230	349	417	464	490
4.2	**2**	164	259	345	403	438

Table 6. Charge readout (nC) by the Advanced Markus dosimeter at 12 MeV energy. (Values are the mean of three repeated measurements (n = 3), rounded to the nearest integer, relative standard deviation (SD= ± 2%).)

Depth of measurement point (cm	Field size (cm^2) / Inhomogeneity (cm)	2×2	3×3	4×4	5×5	6×6
2.7	**0**	381	480	534	565	572
3.2	**0.5**	283	400	472	517	537
3.7	**1**	205	317	400	457	489
4.7	**2**	150	248	331	393	434

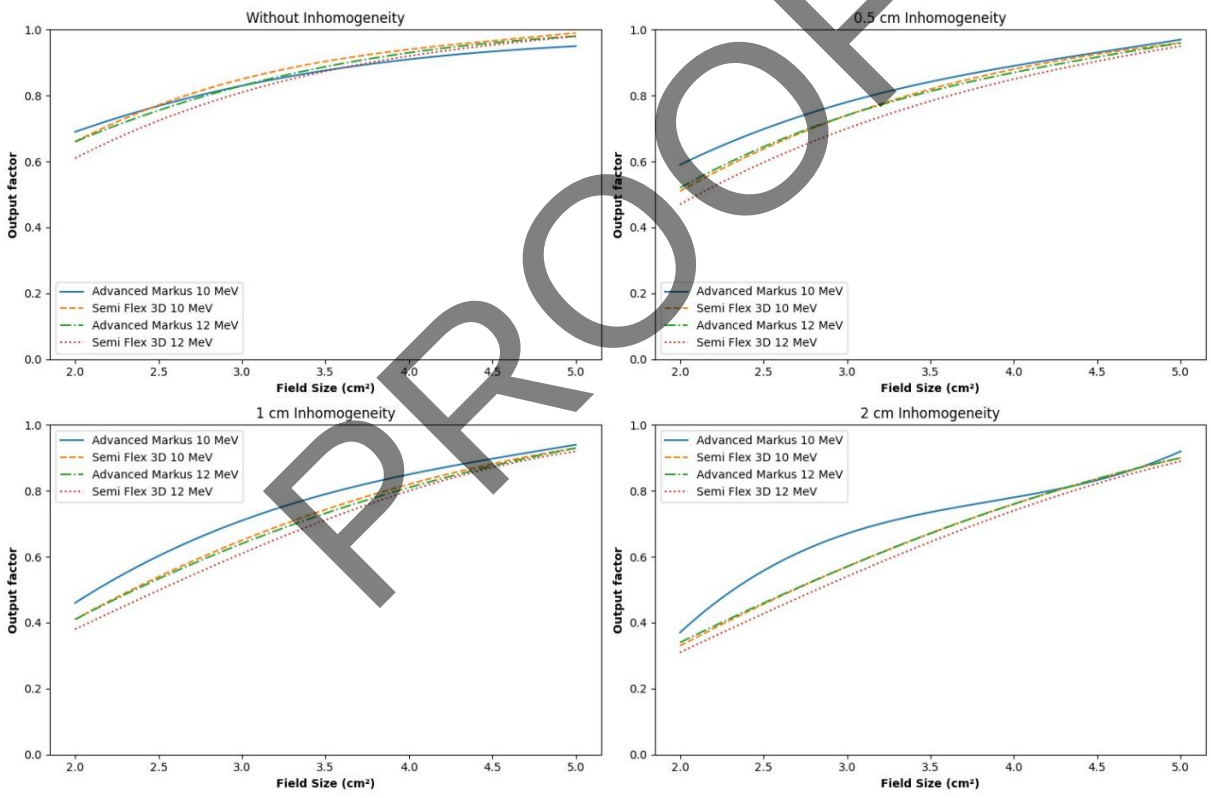

Figure 4. Comparison of Advanced Markus and Semi Flex 3D measurements of OF as a function of field size

Table 7 and Figure 4 illustrate the relationship between field size and OF ($\frac{D_{field}}{D_{ref}}$) for the Advanced Markus and Semi Flex 3D detectors at 10 MeV and 12 MeV, considering different inhomogeneity conditions.

Both detectors demonstrate consistent trends across different field sizes and inhomogeneity levels, suggesting their reliability for measuring electron fields in diverse scenarios. As the inhomogeneity in the chamber increases, the measurement values for both detectors generally decrease. This pattern is consistently observed across all field sizes and energy

Table 7. The OFs values were calculated for Advanced Markus and Semiflex 3D at two energies and different field sizes in the presence of various heterogeneities

Inhomogeneity(cm)	Field size (cm^2)	10 MeV			12 MeV		
		Advanced Markus	Semiflex 3D	Δ(%)	Advanced Markus	Semiflex 3D	Δ(%)
Without Inhomogeneity	2×2	0.69	0.66	0.03	0.66	0.61	0.05
	3×3	0.83	0.85	0.02	0.83	0.81	0.02
	4×4	0.91	0.94	0.03	0.93	0.92	0.01
	5×5	0.95	0.99	0.04	0.98	0.98	0.00
0.5 cm Inhomogeneity in the chamber	2×2	0.59	0.51	0.08	0.52	0.47	0.05
	3×3	0.78	0.74	0.04	0.74	0.70	0.04
	4×4	0.89	0.88	0.01	0.87	0.85	0.02
	5×5	0.97	0.96	0.01	0.96	0.95	0.01
1 cm Inhomogeneity in the chamber	2×2	0.46	0.41	0.05	0.41	0.38	0.03
	3×3	0.71	0.65	0.06	0.64	0.61	0.03
	4×4	0.85	0.82	0.03	0.81	0.80	0.01
	5×5	0.94	0.93	0.01	0.93	0.92	0.01
2 cm Inhomogeneity in the chamber	2×2	0.37	0.33	0.04	0.34	0.31	0.03
	3×3	0.59	0.57	0.02	0.57	0.54	0.03
	4×4	0.78	0.76	0.02	0.76	0.74	0.02
	5×5	0.92	0.90	0.02	0.90	0.89	0.01

levels, emphasizing the detectors' sensitivity to inhomogeneity.

For both detectors, measurement values typically rise with larger field sizes. The reason for this increase is that as the field size grows, the likelihood of lower energy interactions, or in other words, the amount of scattering, increases. This trend holds across varying inhomogeneity conditions and energy levels, indicating that larger field sizes yield higher measurement values. Additionally, measurement values at 12 MeV are usually greater than those at 10 MeV for both detectors; this is again due to the increase in scattering. While both detectors exhibit similar trends, there are minor differences in their measurement values. These insights can enhance our understanding of how detectors behave under various conditions, aiding in the selection of suitable detectors for specific dosimetry applications.

From the data and trends illustrated in Figure 4, we can formulate a general equation that describes the relationship between field size, inhomogeneity, and measurement values for the Advanced Markus and Semi Flex 3D detectors. Let's define F as the field size (in cm^2), I as the inhomogeneity (in cm), and M as the OF. A potential equation to express the OF M could be (Equation 1):

$$M = a.F + b.I + c \quad (1)$$

where a, b, and c are phenomenological parameters. This equation serves as a linear approximation and can be fine-tuned based on the specific data points and trends observed in the figures. To ascertain the precise values of a, b, and c, we conducted a regression analysis of the data. The coefficients were determined to be a=0.13624999999999987, b=-0.0818571428571429, and c= 0.36412500000000037.

The phenomenological coefficients in the Equation 1 M = a F+ b I + c can be interpreted based on the physics of electron beam interactions. Coefficient a reflects the effect of field size on the measured dose, as larger fields increase scattered electrons and consequently the charge collected by the detector. Coefficient b represents the influence of air heterogeneity thickness, with thicker inhomogeneities reducing the measured dose due to decreased electron fluence at the detector. The constant c corresponds to the baseline detector response under reference conditions, i.e., without heterogeneity and at the reference field size. This explanation links the regression model to the observed experimental trends and provides a physical rationale for the parameters derived from the data.

4. Discussion

Accurate dosimetry in small electron fields is crucial for effective radiotherapy, particularly for the

treatment of superficial tumors. Electron beams are commonly used in such cases due to their ability to deliver high doses to surface and near-surface regions while sparing deeper tissues. In this study, cold foam was utilized as a heterogeneous medium because its electron density and Hounsfield Unit (HU) values closely resemble those of air gaps found in treatment areas, such as around the nose or ear in head and neck cancers.

Our results confirm that the OF increases with both field size and beam energy, a trend consistent with previous research showing that larger field sizes enhance lateral electron scatter, leading to higher OF values, while increased beam energy allows for deeper penetration and broader dose distribution, further elevating the OF [2, 10, 11]. Quantitatively, our OF values for 2×2 and 3×3 cm² fields at 10 and 12 MeV were within 2–4% of those reported by Wulandari *et al.* [11], who also observed a strong reduction of OF in sub-3 cm² fields. For larger fields (≥4×4 cm²), our data showed deviations of less than 2% from these published measurements. This indicates that our experimental results are in good agreement with previous electron small-field studies and confirm the reproducibility of OF trends across independent datasets.

To ensure accurate OF measurements in small electron fields, various dosimeters have been utilized. The Semiflex 3D (sensitive volume: 0.07 cm^3) and Advanced Markus (sensitive volume: 0.02 cm^3) ionization chambers are widely recommended for small-field dosimetry due to their high precision and sensitivity to minor variations in dose distribution.

Previous studies have suggested [9, 10] a minimum measurement field size of 3 cm × 3 cm for these detectors. Our findings support this recommendation, as discrepancies between the two dosimeters were observed in 2 cm × 2 cm and 3 cm × 3 cm fields, but for field sizes larger than 3 cm × 3 cm, the differences were minimal, remaining below 2%. This reinforces the reliability of these dosimeters for small-field electron dosimetry.

These results suggest that in clinical practice, caution should be exercised when using electron fields smaller than 3×3 cm² in the presence of air-equivalent heterogeneities, as output factor reductions may lead to underdosing of superficial targets. Treatment planning should account for these effects, and experimental verification is recommended for small-field setups to ensure accurate dose delivery.

Furthermore, this study examined the impact of heterogeneity on the OF. Our results indicate that as the level of heterogeneity increases, the OF measured by both dosimeters decreases. This finding suggests that the presence of air-equivalent heterogeneities leads to a reduction in the OF, an effect consistently observed across all measurements. This reduction was observed across all field sizes and energy levels. For example, in a 3 cm × 3 cm field, the OF decreased from 0.83 (without heterogeneity) to 0.59 (with 2 cm heterogeneity) for the Advanced Markus and 0.85 (without heterogeneity) to 0.57 (with 2 cm heterogeneity) for the semiflex 3D dosimeter at 10 MeV. These changes were similar for 12 MeV as well as for 10 MeV in the 3 cm × 3 cm field, with values decreasing from 0.83 to 0.57 and from 0.81 to 0.54 for the Advanced Markus and Semiflex dosimeters, respectively. Both the Semiflex 3D and Advanced Markus dosimeters confirmed this trend, validating their suitability for small-field electron dosimetry even in the presence of tissue inhomogeneities.

It is also noteworthy that the behavior of our OF measurements aligns with the general framework of IAEA TRS-483. Although TRS-483 primarily guides photon small-field dosimetry, its principles regarding detector correction factors and field output consistency are applicable. Our results are consistent with these recommendations, as deviations between detectors remained below 2% for fields larger than 3×3 cm², comparable to the tolerances suggested in TRS-483. In the computational process of Treatment Planning Systems (TPS), algorithms such as Monte Carlo are widely used to model heterogeneities. In these methods, information regarding material composition and electron density is extracted from CT images and Hounsfield Unit (HU) values. Although these methods are powerful tools due to their high accuracy and ability to simulate the most complex physical conditions, they also have limitations. Firstly, the accuracy of these methods depends on the quality of CT images and the calibration of the CT device. Errors arising from image noise, motion artifacts, or differences in CT device calibration can lead to inaccuracies in determining electron density and material composition. Secondly, the conversion of HU

values to physical parameters is based on simplified models, which may not fully account for the actual variability in the composition of biological tissues.

For example, tissues with similar HU values may have different chemical compositions, which can affect the accuracy of the simulation. Additionally, in highly heterogeneous environments (such as the interface between tissue and air or the presence of metal implants), computational methods may face challenges, as significant variations in density and material composition can lead to errors in dose distribution calculations. Therefore, it is recommended that during the commissioning and data input process for TPS, reliance should not be solely placed on computational methods like Monte Carlo. Instead, the impact of heterogeneities on dose distribution should also be investigated experimentally.

Experimental measurements can serve as effective inputs to the TPS, enhancing the accuracy of computational models. This hybrid approach (combining computational simulations and experimental validation) ensures that treatment planning systems are capable of delivering precise and reliable doses in complex clinical scenarios. Accordingly, it is advised that during the commissioning of TPS in electron mode, OF measurements should include various heterogeneous conditions with different electron densities to ensure comprehensive and clinically accurate dosimetry.

5. Conclusion

Accurate dosimetry in small electron fields is essential for effective radiotherapy, particularly for superficial tumors. This study confirmed that the OF increases with both field size and beam energy, aligning with previous research. Additionally, the presence of air-equivalent heterogeneities was found to decrease the OF, highlighting the importance of considering tissue inhomogeneities in dose calculations. The Semiflex 3D and Advanced Markus ionization chambers proved to be suitable for small-field electron dosimetry, demonstrating high precision and reliability. Given these findings, it is recommended that dosimetric measurements in small electron fields incorporate different heterogeneity conditions. This approach will enhance the accuracy of treatment planning and improve dose delivery in clinical practice.

Acknowledgment

The authors gratefully acknowledge the financial support provided by Arak University of Medical Sciences (Grant No. 7352) for this research.

The studies involving humans were approved by the Ethics Committee of Arak University of Medical Sciences (Approval number IR.ARAKMU.REC.1403.017). The research was carried out in compliance with the regulations of the local jurisdiction and the standards set by the institution.

References

1- Kesen ND, Cakir A, Okutan M, and Bilge H, "A comparison of TPS and different measurement techniques for small-field electron beams." *Medical Dosimetry,* Vol. 40 (No. 1), pp. 9-15, (2015).

2- Russo S *et al.*, "Dosimetric Characterization of Small Radiotherapy Electron Beams Collimated by Circular Applicators with the New Microsilicon Detector." *Applied Sciences,* Vol. 12p. 600, (2022).

3- Ali I, Kendall E, Alsbou N, and Ahmad S, "Quantitative evaluation of the dosimetric uncertainties associated with small electron fields." *Journal of Medical Imaging and Radiation Sciences,* Vol. 53 (No. 2), pp. 273-82, (2022).

4- Van Eeden D, Sachse KN, and Du Plessis FC, "Practical Dosimetry Considerations for Small MLC-Shaped Electron Fields in a 60 cm SSD." *Journal of Biomedical Physics and Engineering,* Vol. 12 (No. 1), pp. 101-08, (2022).

5- Taylor ML, Kron T, and Franich RD, "A contemporary review of stereotactic radiotherapy: inherent dosimetric complexities and the potential for detriment." *Acta Oncologica,* Vol. 50 (No. 4), pp. 483-508, (2011).

6- Khan FM, "Electron Beam Therapy." in *The Physics of Radiation Therapy*, J. W. Pine, Ed. Philadelphia: *Lippincott Williams & Wilkins*, (2010), pp. 256-304.

7- Bagheri H, Soleimani A, Gharehaghaji N, Mesbahi A, Manouchehri F, and Shekarchi B, "An overview of small-field dosimetry in photon beam radiotherapy: Developments and challenges." *Journal of Cancer Research and Therapeutics,* Vol. 13 (No. 2), pp. 175-85, (2017).

8- Gerbi BJ, Antolak JA, Deibel FC, Followill DS, Herman MG, and Higgins PD, "Recommendations for clinical electron beam dosimetry: Supplementary to the

recommendations of Task Group 25." *Medical Physics,* Vol. 36 (No. 7), pp. 3239-79, (2009).

9- International Atomic Energy Agency, "Absorbed Dose Determination in External Beam Radiotherapy." *IAEA*, Vienna, Austria, (2000).

10- Donmez Kesen N, Cakir A, Okutan M, and Bilge H, "Research of dosimetry parameters in small electron beams." *Science and Technology of Nuclear Installations,* Vol. 2014 (No. 1), p. 585219, (2014).

11- Wulandari C, Wibowo WE, and Pawiro SA, "The detector characteristics for output factor measurement of small field electron beams." Presented at the *AIP Conference Proceedings*, (2017).